



This article appeared in a journal published by Elsevier. The attached copy is furnished to the author for internal non-commercial research and education use, including for instruction at the authors institution and sharing with colleagues.

Other uses, including reproduction and distribution, or selling or licensing copies, or posting to personal, institutional or third party websites are prohibited.

In most cases authors are permitted to post their version of the article (e.g. in Word or Tex form) to their personal website or institutional repository. Authors requiring further information regarding Elsevier's archiving and manuscript policies are encouraged to visit:

<http://www.elsevier.com/copyright>



Contents lists available at ScienceDirect

Thin Solid Films

journal homepage: www.elsevier.com/locate/tsfParameterization of $\text{CuIn}_{1-x}\text{Ga}_x\text{Se}_2$ ($x = 0, 0.5$, and 1) energy bandsRongzhen Chen^{*}, Clas Persson

Department of Materials Science and Engineering, Royal Institute of Technology, SE-100 44 Stockholm, Sweden

ARTICLE INFO

Available online 13 January 2011

Keywords:

CuInSe_2
 CuGaSe_2
 Chalcopyrite
 Solar cells
 Band structure
 Electronic structure
 Effective mass

ABSTRACT

Parameterization of the electronic band structure of $\text{CuIn}_{1-x}\text{Ga}_x\text{Se}_2$ ($x = 0, 0.5$, and 1) demonstrates that the energy dispersions of the three uppermost valence bands [$E_j(\mathbf{k})$; $j = v1, v2$, and $v3$] are strongly anisotropic and non-parabolic even very close to the Γ -point valence-band maximum $E_{v1}(\mathbf{0})$. Also the lowest conduction band $E_{c1}(\mathbf{k})$ is anisotropic and non-parabolic for energies ~ 0.05 eV above the band-gap energy. Since the electrical conductivity depends directly on the energy dispersion, future electron and hole transport simulations of $\text{CuIn}_{1-x}\text{Ga}_x\text{Se}_2$ need to go beyond the parabolic approximation of the bands. We therefore present a parameterization of the energy bands, the \mathbf{k} -dependency of the effective electron and hole masses $m_j(\mathbf{k})$, and also an average energy-dependent approximation of the masses $m_j(E)$.

© 2011 Elsevier B.V. All rights reserved.

1. Introduction

The effective electron and hole masses $m_j(\mathbf{k})$ are very often utilized to represent the shape of the energy bands, thus assuming parabolic energy dispersion. However, typically these effective masses describe the energy bands only near the considered \mathbf{k} -point, whereas away from this point the bands can be strongly non-parabolic. If the non-parabolicity occurs within the energy region of temperature statistics (~ 0.03 eV), band-filling effects (~ 0.1 eV) or sunlight absorption and hot electron transport (~ 0.5 eV), the exact shape of the bands has to be considered when analyzing modeled and measured results involving for instance electron transport or band filling of the materials.

In this work, we have parameterized the lowest conduction band (CB) and the three uppermost valence bands (VBs) of $\text{CuIn}_{1-x}\text{Ga}_x\text{Se}_2$ ($x = 0, 0.5$, and 1 ; thus CuInSe_2 , $\text{CuIn}_{0.5}\text{Ga}_{0.5}\text{Se}_2$, and CuGaSe_2) in order to better describe the non-parabolic and anisotropy of the energy bands $E_j(\mathbf{k})$. We report that the three topmost VBs ($E_j(\mathbf{k})$ with $j = v1, v2$, and $v3$) are very non-parabolic and anisotropic for energies $E_j(\mathbf{k}) < E_{v1}(\mathbf{0}) - 0.01$ eV. This non-parabolicity is mainly due to the split of degeneracy caused by the spin-orbit and crystal-field interactions. Also the lowest CB ($j = c1$) starts to become non-parabolic and anisotropic for energies above $E_{c1}(\mathbf{k}) > E_{c1}(\mathbf{0}) + 0.05$ eV. However, this non-parabolicity is a normal effect of the Bloch-periodic crystal potential. With the parameterized energy dispersion, the \mathbf{k} -dependent electron and hole masses are analyzed, and especially the hole masses of the two topmost VBs show a strong \mathbf{k} -dependency. We also present an energy-dependent approximation of the masses $m_j(E)$ that can be used in already existing analysis methods involving the parabolic approximation and/or strong band-filling effects.

2. Parameterization of the energy bands

The employed electronic band structure originates from an all-electron and full-potential linearized augmented plane wave calculation [1,2] using the Engel–Vosko (EV) exchange–correlation potential within the generalized gradient approximation [3]. We have recently shown [4] that the regular local density approximation (LDA) underestimates the effective masses for materials with small direct energy gaps; this is due to a too strong coupling between the CB and VBs. For GaAs for instance (which is the group-III–V analogue to CuGaSe_2 , having also similar band-gap energies), the measured Γ -point electron mass is $m_c = 0.067 m_0$, the heavy-hole mass (averaged over \mathbf{k} -direction) is $m_{hh} = 0.51 m_0$, the light-hole mass is $m_{lh} = 0.08 m_0$, and the spin-orbit split-off hole mass is $m_{sh} = 0.15 m_0$ [5]. LDA underestimates the masses [6]: $m_c = 0.018 m_0$, $m_{hh} = 0.55 m_0$, $m_{lh} = 0.01 m_0$, and $m_{so} = 0.08 m_0$, whereas the EV potential generates much more accurate masses [6]: $m_c = 0.061 m_0$, $m_{hh} = 0.55 m_0$, $m_{lh} = 0.07 m_0$, and $m_{so} = 0.16 m_0$. The reason for the improved energy dispersion of the EV potential is that this exchange–correlation model generates better interaction potentials but less accurate total energies compared with LDA.

The employed calculation from Refs. [1] and [2] shows (solid lines in Fig. 1) that the VBs are anisotropic in an energy region about 0.0–1.0 eV below the VB maximum (VBM). In the (110) and (112) directions the two uppermost VBs are very flat, and they reach the Brillouin zone (BZ) edge at about -0.5 eV. A closer look at the VBM (Fig. 2; solid lines) reveals that the energy bands start to become very non-parabolic already in the 0.01–0.1 eV region below VBM. The parabolic approximation of ellipsoidal energy bands reads

$$E_j^{pb}(\mathbf{k}) = E_j(\mathbf{0}) \pm \left[\frac{\tilde{k}_x^2 + \tilde{k}_y^2}{m_j^\perp} + \frac{\tilde{k}_z^2}{m_j^\parallel} \right] \quad \text{with} \quad \tilde{k}_\alpha^2 = \frac{\hbar^2 k_\alpha^2}{2e}, (\alpha = x, y \text{ and } z), \quad (1)$$

^{*} Corresponding author.E-mail address: rche@kth.se (R. Chen).

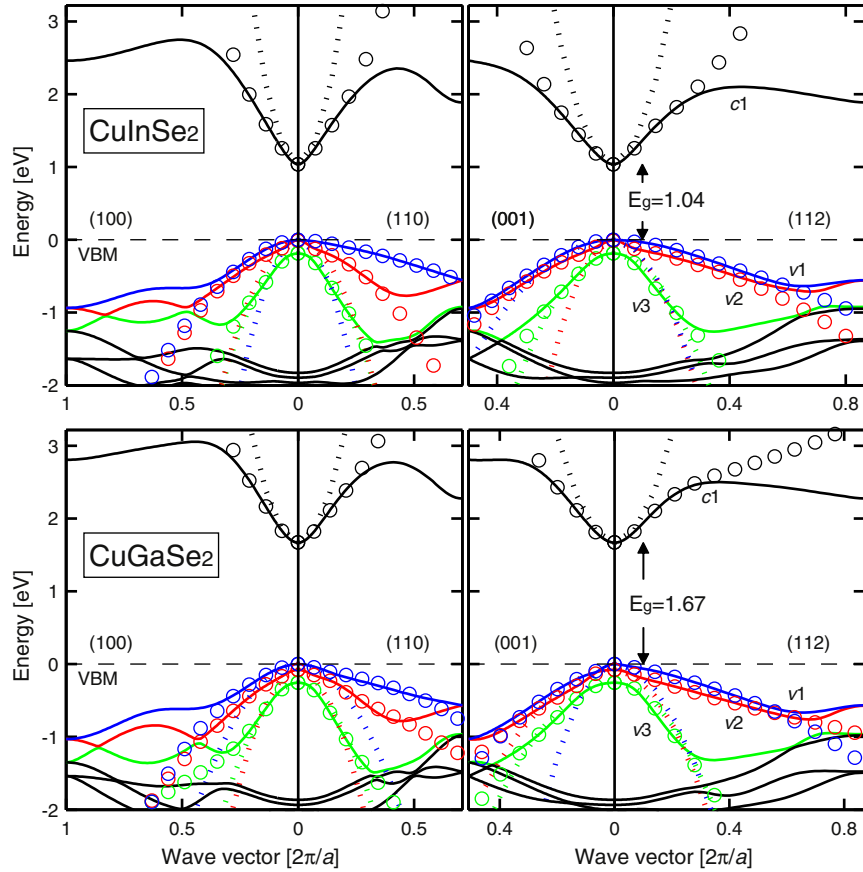


Fig. 1. Electronic band structure $E_j(\mathbf{k})$ of CuInSe_2 (upper panels) and CuGaSe_2 (lower panels) along the four symmetry directions (100), (110), (001), and (112). The energies referred to the VBM (dashed lines). The notation of the energy bands ($j = c1, v1, v2$, and $v3$) at the band edges refers to a spin-independent band indexing, where $c1$ represents the lowest CB and $v1$ represents the topmost VB. These VBs are highlighted with colors in the online version. The solid lines show the full-potential results from Refs. [1] and [2], the dotted lines represent the parabolic approximation of Eq. (1), and the circles are the fitted results of Eq. (2). Notice that the two uppermost VBs are badly described by the parabolic approximation in the main (100), (110), and (112) symmetry directions. Here, the notation of the symmetry directions (k_x, k_y , and k_z) is in units of $2\pi/a$, $2\pi/a$, and $2\pi/c$.

where e is the elementary charge and positive (negative) sign is for the CB (VBs). We have verified in this study that the ellipsoidal energy dispersion (Table 1) is valid for all four considered energy bands ($j = c1, v1, v2$, and $v3$) in the very vicinity of the Γ -point. However, away from the Γ -point, the parabolic approximation (dotted lines in Figs. 1 and 2) obviously fails to describe the energy dispersion of the VBs, especially for the topmost band in the (110) and (112) directions.

A common way to parameterize the energy bands is within the so called $\mathbf{k} \cdot \mathbf{p}$ approximation [7]. For cubic materials with twofold degenerate cation- s -anion- p bonding-like VBM the (spin-independent) energy dispersion has the form [7,8] $E_j(\mathbf{k}) = E_j^{pb}(\mathbf{k}) \pm \Delta \cdot (\delta \cdot (k_x^2 k_y^2 + k_y^2 k_z^2 + k_z^2 k_x^2) + k^4)^{1/2}$, and the corresponding expression for hexagonal structure is of the form $E_j(\mathbf{k}) = E_j^{pb}(\mathbf{k}) \pm \Delta \cdot (\delta \cdot k_\perp^4 + 1)^{1/2}$. However, the disadvantage with this method is that even for rather simple materials (like cubic or hexagonal SiC [8]) the parameterized bands can describe the VBs only close to the Γ -point. $\text{CuIn}_{1-x}\text{Ga}_x\text{Se}_2$ has a VBM involving Cu- d -Se- p antibonding-like state, and the crystal-field interaction as well as the spin-orbit coupling generates rather complex (anisotropic and non-parabolic) energy dispersions (Figs. 1 and 2). Therefore, the regular $\mathbf{k} \cdot \mathbf{p}$ approximation is not a sufficient method for describing the energy bands of $\text{CuIn}_{1-x}\text{Ga}_x\text{Se}_2$ down to ~ 0.5 eV below VBM. Instead, we start extend the $\mathbf{k} \cdot \mathbf{p}$ expressions to higher orders and with lower band symmetries, choosing the form $E_j(\mathbf{k}) = E_j^{pb}(\mathbf{k}) + \sum_{\alpha,n} \Delta_{\alpha,n} \cdot (\delta_{\alpha,n} \cdot k_\alpha^{2n} + 1)^{1/n}$. Each term alone describes a parabolic dispersion, but the higher order terms affect the dispersion for the larger wave vectors away from the

Γ -point. Thus, the combination of terms can therefore describe how local effects (like crystal field and spin-orbit coupling) re-shape the energy dispersion, that otherwise would be parabolic. We find that the following expression is suitable to describe the energy bands of $\text{CuIn}_{1-x}\text{Ga}_x\text{Se}_2$ down to ~ 0.5 eV below VBM:

$$E_j(\mathbf{k}) = E_j^{pb}(\mathbf{k}) + E_j^0 + \Delta_{j,1} \left(\delta_{j,1}^2 \left(\frac{\tilde{k}_x^4 + \tilde{k}_y^4}{m_0^2} \right) + \delta_{j,2}^2 \left(\frac{\tilde{k}_x^2 \tilde{k}_y^2}{m_0^2} \right) + 1 \right)^{1/2} \\ + \Delta_{j,2} \left(\delta_{j,3}^3 \left(\frac{\tilde{k}_x^6 + \tilde{k}_y^6}{m_0^3} \right) + \delta_{j,4}^3 \left(\frac{\tilde{k}_x^2 \tilde{k}_y^4 + \tilde{k}_x^4 \tilde{k}_y^2}{m_0^3} \right) + 1 \right)^{1/3} \\ + \Delta_{j,3} \left(\delta_{j,5}^2 \left(\frac{\tilde{k}_z^4}{m_0^2} \right) + 1 \right)^{1/2} + \Delta_{j,4} \left(\delta_{j,6}^3 \left(\frac{\tilde{k}_z^6}{m_0^3} \right) + 1 \right)^{1/3} \\ + \Delta_{j,5} \left(\delta_{j,7}^2 \left(\frac{\tilde{k}_x^2 \tilde{k}_z^2 + \tilde{k}_y^2 \tilde{k}_z^2}{m_0^2} \right) + 1 \right)^{1/2} \\ + \Delta_{j,6} \left(\delta_{j,8}^3 \left(\frac{\tilde{k}_x^4 \tilde{k}_z^2 + \tilde{k}_y^4 \tilde{k}_z^2}{m_0^3} \right) + \delta_{j,9}^3 \left(\frac{\tilde{k}_x^2 \tilde{k}_z^4 + \tilde{k}_y^2 \tilde{k}_z^4}{m_0^3} \right) + \delta_{j,10}^3 \left(\frac{\tilde{k}_x^2 \tilde{k}_y^2 \tilde{k}_z^2}{m_0^3} \right) + 1 \right)^{1/3}. \quad (2)$$

Unfortunately, the rather complex VB energy dispersions of $\text{CuIn}_{1-x}\text{Ga}_x\text{Se}_2$ require quite many fitting parameters (Eq. (2) and Table 2). The CB, however, needs less parameters.

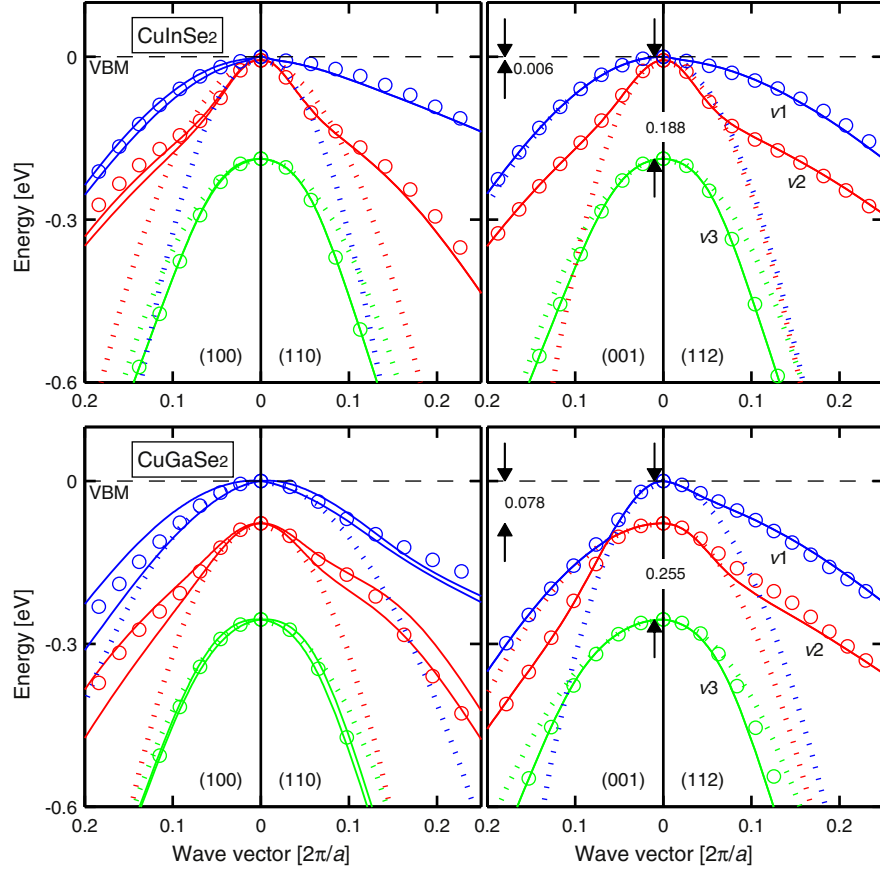


Fig. 2. Close-up of Fig. 1 demonstrating the strong non-parabolicity of the topmost VBs. Our parameterized energy bands $E_j(\mathbf{k})$ consider the average of the two spinor states $\psi_j^{\sigma}(\mathbf{k})$ with $\sigma = \uparrow$ and \downarrow , although there is a relatively large split of the spin-up- and spin-down-like bands in the (100)-direction; this average approximation is justified by $\psi_j^{\sigma}(-\mathbf{k}) = \psi_j^{\sigma}(\mathbf{k})$. Thus, the notation of the energy bands is $j = c1, v1, v2$, and $v3$ (where $c1$ represents the lowest CB and $v1$ represents the topmost VB) refers to a spin-independent band indexing.

Table 1

Parameters of Eq. (1) to describe the parabolic energy dispersions of the lowest CB and the three uppermost VBs in the vicinity of the Γ -point. $E_{v1}(\mathbf{0})$ is the VBM and $E_{c1}(\mathbf{0})$ is the fundamental band-gap energy E_g .

CuIn _{1-x} Ga _x Se ₂	x = 0.0				x = 0.5				x = 1.0			
	c1	v1	v2	v3	c1	v1	v2	v3	c1	v1	v2	v3
$E_j(\mathbf{0})$ [eV]	0.97	0.00	0.01	0.19	1.20	0.00	0.02	0.20	1.47	0.00	0.08	0.26
$m_{j\perp}^{\perp}$ [m_0]	0.08	0.14	0.25	0.27	0.10	0.40	0.17	0.29	0.13	0.47	0.20	0.29
m_j^{\parallel} [m_0]	0.09	0.66	0.12	0.28	0.11	0.14	0.61	0.40	0.13	0.15	0.61	0.49

Table 2

Parameters of Eq. (2) to describe the non-parabolic contribution to the energy dispersions $E_j(\mathbf{k})$ of the lowest CB and the three uppermost VBs. The notation of the energy bands ($j = c1, v1, v2$, and $v3$) refers to a spin-independent band indexing, where $c1$ represents the bottommost CB and $v1$ represents the topmost VB (see Figs. 1 and 2).

CuIn _{1-x} Ga _x Se ₂	x = 0.0				x = 0.5				x = 1.0			
	c1	v1	v2	v3	c1	v1	v2	v3	c1	v1	v2	v3
E_j^0 [eV]	-4.010	-5.311	-5.242	-5.620	-4.146	-6.210	-6.426	-5.835	-3.927	5.284	-5.789	-2.783
Δ_{j1} [eV]	-0.295	0.006	-0.002	-0.021	-0.230	0.106	1.321	-0.026	-0.454	0.116	1.284	1.194
Δ_{j2} [eV]	0	0.098	0.104	0.308	0	0.002	0.096	0.386	0	-10.771	-0.837	-0.024
Δ_{j3} [eV]	-0.242	0.018	0.124	-0.025	-0.293	0.937	-0.017	-0.838	-0.419	0.088	0.347	-0.303
Δ_{j4} [eV]	0	0.188	0.076	0.238	0	0.021	0.163	0.789	0	0.076	-0.051	0.608
Δ_{j5} [eV]	-0.016	-0.048	0.001	-0.009	-0.046	0.001	0.011	0.370	-0.047	0.022	0.274	0.374
Δ_{j6} [eV]	0	0.037	-0.073	0.117	0	-0.022	-0.313	-0.012	0	-0.111	-0.525	-4.362
δ_{j1} [eV ⁻¹]	30.669	952.000	2304.147	94.139	27.157	5.517	1.029	57.007	11.865	10.526	9.269	3.839
δ_{j2} [eV ⁻¹]	47.374	1754.386	4587.156	220.556	44.506	13.610	0.413	153.435	20.262	28.545	21.582	6.232
δ_{j3} [eV ⁻¹]	0	3.970	72.296	11.746	0	487.805	46.950	8.489	0	0.131	9.116	59.625
δ_{j4} [eV ⁻¹]	0	3.688	123.274	18.078	0	1128.668	72.844	13.509	0	0.126	21.328	148.516
δ_{j5} [eV ⁻¹]	31.852	6.041	56.004	64.137	21.124	1.314	247.158	7.921	12.978	7.709	12.141	8.014
δ_{j6} [eV ⁻¹]	0	3.134	6.100	12.031	0	267.523	29.076	8.743	0	64.185	66.808	5.309
δ_{j7} [eV ⁻¹]	222.641	37.004	3846.154	206.148	79.879	3322.259	212.902	16.836	76.319	236.742	16.240	5.092
δ_{j8} [eV ⁻¹]	0	12.647	16.269	6.982	0	92.954	4.885	57.890	0	31.947	6.710	1.209
δ_{j9} [eV ⁻¹]	0	61.565	33.169	34.114	0	118.064	0.000	273.400	0	34.784	4.831	1.394
δ_{j10} [eV ⁻¹]	0	46.679	31.275	32.237	0	110.327	6.074	153.523	0	40.765	5.243	2.124

The parameterized energy bands (circles in Figs. 1 and 2) can fairly accurately describe the energy bands for energies ~ 0.5 eV below the VBM and ~ 0.5 eV above the CB minimum (CBM). The energy difference of the two uppermost VBs at the Γ -point is only $E_{v1}(\mathbf{0}) - E_{v2}(\mathbf{0}) = 6, 18,$ and 78 meV for CuInSe_2 , $\text{CuIn}_{0.5}\text{Ga}_{0.5}\text{Se}_2$, and CuGaSe_2 , respectively. These two VBs interact in this energy region which affects the band curvatures, and thus making the bands non-parabolic and anisotropic. Therefore, the parabolic approximation (represented by the Γ -point effective hole masses) is strictly valid only for energies to about $-4, -10,$ and -40 meV below the VBM for CuInSe_2 , $\text{CuIn}_{0.5}\text{Ga}_{0.5}\text{Se}_2$, and CuGaSe_2 , respectively (see Fig. 2).

The CB has a rather spherical energy dispersion close to the Γ -point (i. e., $m_{c1,\perp} \approx m_{c1,\parallel}$; [1]). Since the CB is a single band, it is expected that the band is more parabolic and isotropic compared with the VBs. This is true, but already at an energy about 0.05 eV above the CBM $E_{c1}(\mathbf{0})$, the

band becomes both non-parabolic and anisotropic (e. g. Fig. 1). This is a consequence of the crystal potential that makes the CB flat at about 50% out from the Γ -point in the first BZ. Our fitting using Eq. (2) can describe this non-parabolicity and the anisotropy to describe the CB to about $\sim 50\%$ of the first BZ. However, the fitting cannot describe the flat curvature in the remaining part of the BZ in especially the (100) direction.

3. Effective electron and hole masses

From the parameterized energy bands of Eq. (2), the effective electron and hole mass tensors $m_j(\mathbf{k}) = \pm \hbar^2 / (\partial^2 E_j(\mathbf{k}) / \partial \mathbf{k}^2)|_{\mathbf{k}}$ were determined along the four symmetry directions. In Fig. 3, we present the inverse of the mass $m_j(\mathbf{k})^{-1}$ for better visibility; for instance, the mass goes to infinity (whereas inverse mass is zero) when the energy

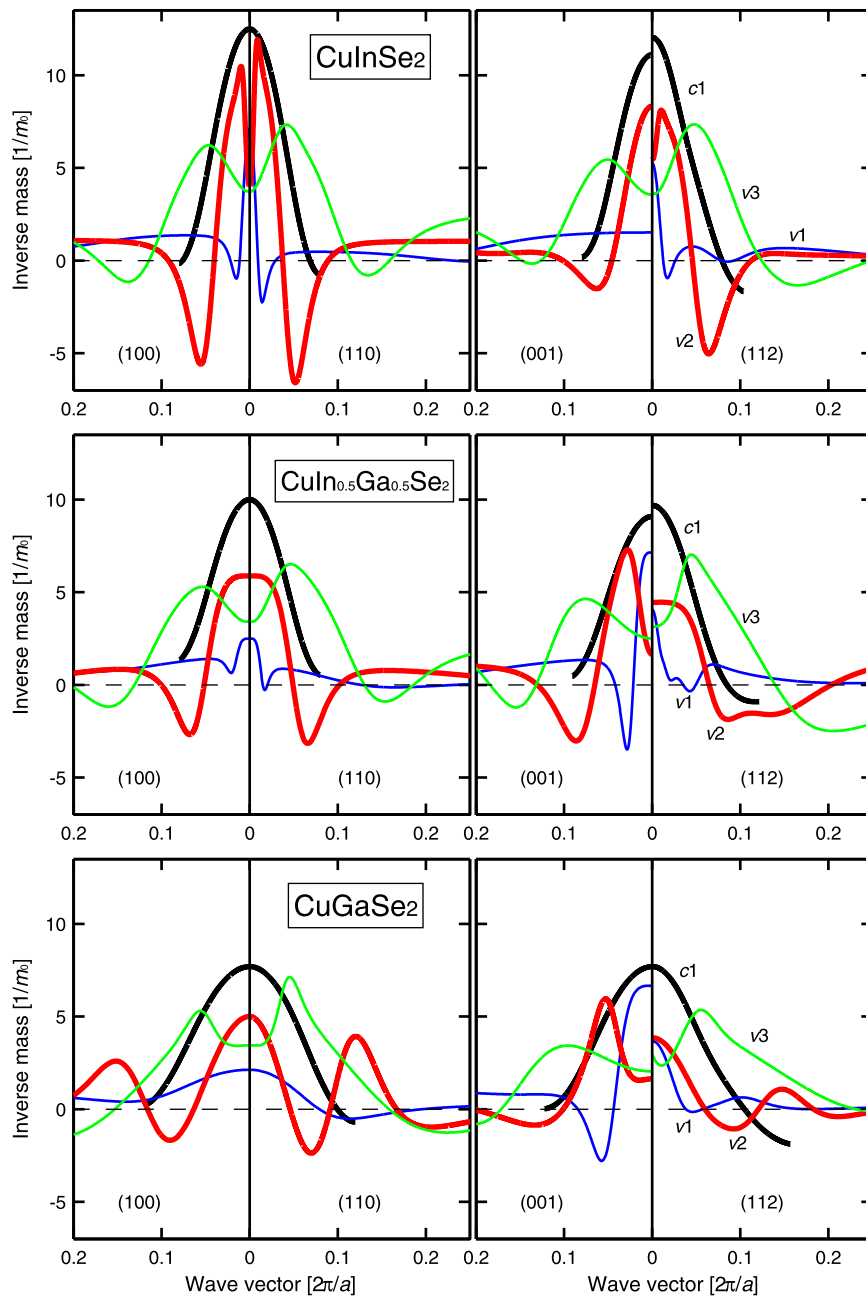


Fig. 3. Inverse of the effective electron and hole masses for $\text{CuIn}_{1-x}\text{Ga}_x\text{Se}_2$ ($x = 0, 0.5,$ and 1) in the four symmetry directions as in Fig. 2, obtained from the second derivative of the energy dispersion: $m_j(\mathbf{k})^{-1} = \pm (\partial^2 E_j(\mathbf{k}) / \partial \mathbf{k}^2) / \hbar^2$. The band indices ($j = c1, v1, v2,$ and $v3$) refer to the energy bands in Figs. 1 and 2. The presented masses are the component parallel to the considered symmetry directions.

dispersion $E_j(\mathbf{k})$ is linear with respect to \mathbf{k} . Fig. 3 demonstrates a strong non-parabolicity of all the considered bands, that is, $m_j(\mathbf{k})^{-1}$ is not constant along each symmetry direction. Moreover, it is clear from the figure that the CB has a rather isotropic electron mass tensor at the Γ -point [thus, $m_{c1}^{100}(\mathbf{0}) \approx m_{c1}^{110}(\mathbf{0}) \approx m_{c1}^{001}(\mathbf{0}) \approx m_{c1}^{112}(\mathbf{0})$]; this is especially true for CuGaSe₂ whereas the electron mass of CuInSe₂ is somewhat anisotropic, as discussed also in Ref. [1]. The effective hole masses of the two topmost VBs ($j = v1$ and $v2$) show very strong anisotropy at the Γ -point [e.g., $m_{v1}^{100}(\mathbf{0}) \neq m_{v1}^{001}(\mathbf{0}) \neq m_{v1}^{112}(\mathbf{0})$]. However, for all bands and at the Γ -point, the inverse mass in the (110)-direction equals the inverse mass in the (100)-direction [thus, $m_j^{100}(\mathbf{0}) = m_j^{110}(\mathbf{0})$], conforming that we can use the notation transverse mass $m_j^{\perp} \equiv m_j^{100}$ and longitudinal mass $m_j^{\parallel} \equiv m_j^{001}$ at the Γ -point.

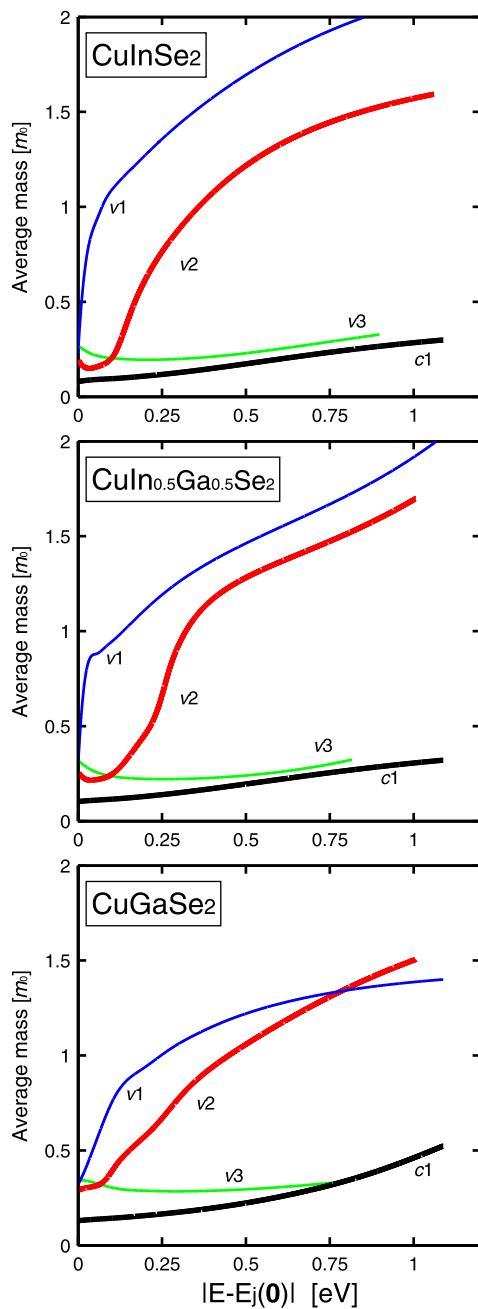


Fig. 4. The average energy-dependent masses of CuIn_{1-x}Ga_xSe₂ ($x = 0, 0.5$, and 1) to be used in analysis methods involving the parabolic approximation: $m_j(E) = \hbar^2(3\pi^2N/V)^{2/3}/2|E - E_j(\mathbf{0})|$, where N is the number of energy states inside the constant energy surface for a crystal with volume V . The band indices ($j = c1, v1, v2$, and $v3$) refer to the energy bands in Figs. 1 and 2.

At the very Γ -point, the values of the electron masses $m_{c1}(\mathbf{k} = \mathbf{0})$ in Table 1 confirm our earlier theoretical results [1]. Moreover, for CuInSe₂ the calculated electron mass components $m_{c1}^{\perp} = 0.08 m_0$ and $m_{c1}^{\parallel} = 0.09 m_0$ verify the Faraday rotation data by Weinert et al. [9] $m_{c1} = 0.09 m_0$ and Shubnikov-de Haas oscillation data by Arushanov et al. [10] $m_{c1} = 0.08 m_0$. However, from Fig. 3, it is clear that the effective electron mass increases (i.e., inverse mass decreases) away from the Γ -point. This will affect the electron transport properties at high electric applied field. At $|\mathbf{k}| \approx 0.1 \cdot 2\pi/a$ the mass is infinity (i.e., $m_j(\mathbf{k})^{-1} = 0$). This occurs at about 0.3 eV above the CBM, reflecting that the CB starts to become more flat with a negative mass further out in the BZ (see Fig. 1). Our parameterized energy dispersion describes this effect on the mass, but it cannot describe the negative electron mass for $|\mathbf{k}| > 0.15 \cdot 2\pi/a$.

Since the spin-orbit coupling and the crystal field affect the VB curvatures near the Γ -point primarily, the uppermost VBs are strongly non-parabolic (Fig. 2), and this will directly affect the effective hole masses (Fig. 3). Hole masses of CuGaSe₂ vary somewhat less compared with those of CuInSe₂, mainly because CuGaSe₂ has larger split between the VBs. Overall, all the three CuIn_{1-x}Ga_xSe₂ compositions show comparable \mathbf{k} -dependency of their masses.

Due to the strong non-parabolicity, the Γ -point hole masses are strictly valid only close to the Γ -point, and can therefore not be used to describe band filling. We therefore present also an average energy-dependent effective mass $m_j(E)$ that can be employed in future analysis (Fig. 4). This mass can thus describe the quasi Fermi level $|E - E_j(\mathbf{0})|$ as function of band filling. From the figure, it is clear that one needs to consider the non-parabolicity of the two uppermost VBs when to analyze hole transport or band filling effects. For instance, $m_{v1}^{\perp} = 0.14 m_0$ and $m_{v1}^{\parallel} = 0.66 m_0$ in CuInSe₂ yield $m_{v1}(E \approx 0) = (m_{v1}^{\perp} m_{v1}^{\parallel})^{1/3} = 0.23 m_0$. This mass increases drastically when E increases to about $1.00 m_0$ at $E = 0.1$ eV. This can thus explain the large measured hole masses $m_{v1} \approx 0.7 m_0$ in CuInSe₂ [11,12] since the indirect measurements involves high hole concentrations. Also analyses involving band filling of the CB need to consider the non-parabolicity since the $m_{c1}(E)$ is increased by about a factor of 2 at energy $|E - E_{c1}(\mathbf{0})| = 0.5$ eV.

4. Summary

To summarize, the parameterization of the electronic band structure of CuIn_{1-x}Ga_xSe₂ ($x = 0, 0.5$, and 1) demonstrates that the energy dispersions of the lowest CB and uppermost VBs [that is, $E_j(\mathbf{k})$ with $j = v1, v2$, and $v3$] are strongly anisotropic and non-parabolic close to the Γ -point VB $E_{v1}(\mathbf{0})$. This anisotropy and non-parabolicity directly affect the effective electron and hole masses.

Acknowledgements

This work is supported by the Swedish Energy Agency, the Swedish Research Council, the China Scholarship Council, and the computers centers NSC and HPC2N through SNIC/SNAC.

References

- [1] C. Persson, Appl. Phys. Lett. 93 (2008) 072106.
- [2] C. Persson, Thin Solid Films 517 (2009) 2374.
- [3] E. Engel, S.H. Vosko, Phys. Rev. B 47 (1993) 13164.
- [4] C. Persson, S. Mirbt, Br. J. Phys. 36 (2006) 286.
- [5] O. Madelung (Ed.), Semiconductors - Basic Data, 2nd ed., Springer, Berlin, 1996.
- [6] C. Persson, R. Ahuja, B. Johansson, Phys. Rev. B 64 (2001) 033201.
- [7] J.M. Luttinger, W. Kohn, Phys. Rev. 97 (1955) 869.
- [8] C. Persson, U. Lindefelt, J. Appl. Phys. 82 (1997) 5496.
- [9] H. Weinert, H. Neumann, H.-J. Höbner, G. Kühn, N. van Nam, Phys. Status Solidi B 81 (1977) K59.
- [10] E. Arushanov, L. Essaleh, J. Galibert, J. Leotin, M.A. Arsene, J.P. Peyrade, S. Askenazy, Appl. Phys. Lett. 61 (1992) 958.
- [11] N.N. Syrbu, I.M. Tiginyanu, L.L. Nemerenco, V.V. Ursaki, V.E. Tezlevan, V.V. Zalamai, J. Phys. Chem. Solids 66 (2005) 1974.
- [12] H. Neumann, W. Kissinger, H. Sobotta, V. Riede, G. Kühn, Phys. Status Solidi B 108 (1981) 483.